

Global Electron Energy Confinement of Neon Plasmas in LHD

J. Miyazawa, H. Yamada, S. Morita, Y. Takeiri, M. Osakabe, K. Narihara, K. Tanaka, S. Sakakibara, M. Goto, S. Murakami, R. Sakamoto, B.J. Peterson, K. Ida, O. Kaneko, K. Kawahata, A. Komori, Y. Nakamura, N. Ohyabu, and LHD experimental Group
National Institute for Fusion Science, 322-6 Oroshi-cho, Toki, Gifu 509-5292, Japan

Neon gas puff experiment has been performed on the Large Helical Device (LHD), to investigate the effect of electric charge and mass of plasma ions on the energy confinement property. Here, we focus on the global energy confinement of electrons in the plasmas heated by the neutral beam (NB) injection. The major radius of the magnetic axis, R , and the plasma minor radius, a , are fixed to 3.6 m and 0.62 m, respectively. Meanwhile, the magnetic field strength at the plasma center, B_0 , is changed from 1.5 T to 2.893 T.

The relation between the electron (ion) temperature at the plasma center, T_{e0} (T_{i0}), and the volume averaged electron density, $\langle n_e \rangle$, is plotted in Fig. 1 (a) (Fig. 1 (b)). Only the hydrogen (or the neon) gas is puffed into plasmas denoted as ‘hydrogen’ (or, ‘neon’) plasmas. The highest T_{e0} is obtained in the neon plasmas, although the difference from the hydrogen data is not remarkable. As for the T_{i0} , which is plotted in Fig. 1 (b), there is a significant difference between the hydrogen plasmas and the neon plasmas; i.e. T_{i0} of the neon plasmas is more than 1.5 times higher than that of the hydrogen plasmas, in the high B_0 case. In Fig. 1 (c), drawn is the $\langle n_e \rangle$ dependence of the electron-stored energy, W_{e_kin} , which is estimated from the profiles of $T_e(\rho)$ and $n_e(\rho)$, where $\rho = r/a$ is the normalized radius. The energy confinement time of the helical plasmas usually exhibits the positive dependence on density as summarized in the international stellarator scaling 95 (ISS95) [1]. In the experiment, the positive density dependence of W_{e_kin} can be recognized only in the low-density regime of $\langle n_e \rangle < 2 \times 10^{19} \text{ m}^{-3}$ (see Fig. 1 (c)). This ‘saturation’ of the global confinement in the high-density regime is not fully understood at this moment. In this study, however, our interest lies in the difference between the hydrogen plasmas and the neon plasmas. Therefore, we restrict the density range as $\langle n_e \rangle < 2 \times 10^{19} \text{ m}^{-3}$ in the analysis below, to eliminate the saturated data.

In LHD, negative-ion based NB injection systems are adopted and the energy of the beam ions, E_{NB} , is much larger than T_e (typically, $E_{NB} > 150 \text{ keV}$). This results in the large fraction of the electron heating power, P_{NB_e} , of about $0.8 P_{NB}$. Here, ‘pure’ plasmas are assumed for both of the hydrogen ($Z_{eff} = 1$) and the neon ($Z_{eff} = 10$), to give P_{NB_e} . As seen in Fig. 1 (a) and (b), $T_{i0} < T_{e0}$ is observed in the low-density hydrogen plasmas, and therefore

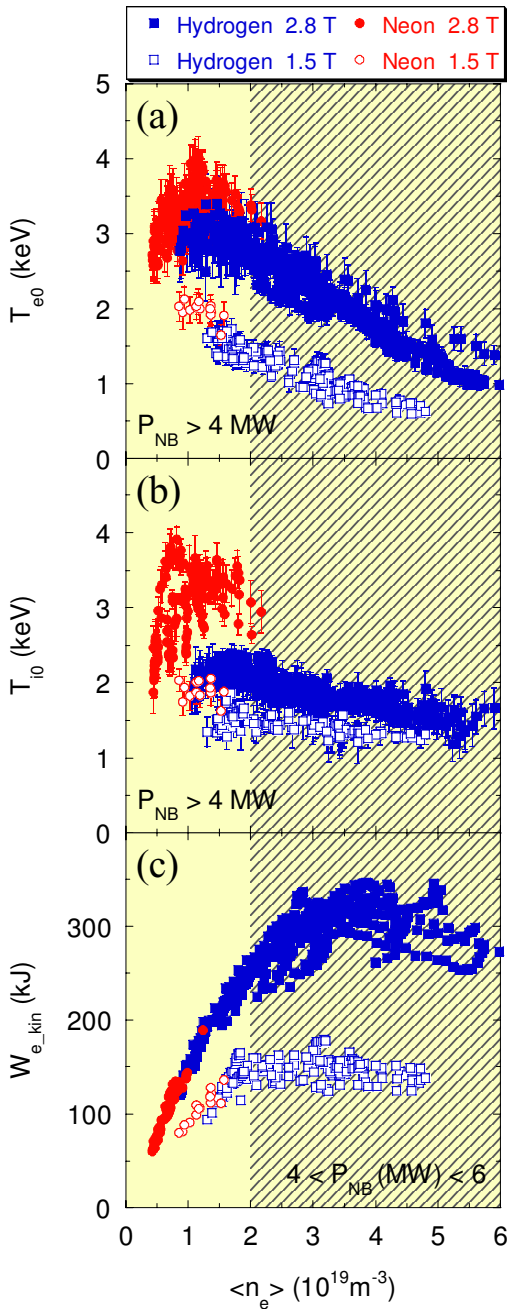


Fig. 1. Distributions of (a) T_{e0} , (b) T_{i0} , and (c) W_{e_kin} , with respect to $\langle n_e \rangle$.

differences between the hydrogen and the neon plasmas can be recognized. The maximum T_{e0} obtained in the neon plasmas can be attributed to the increased heating power due to the small fraction of the NB shine-through power at the low-density regime. Above $P_{NB_e} / \langle n_e \rangle > 5 \text{ MW} / 10^{19} \text{ m}^{-3}$, however, T_{e0} gradually decreases. The reason why this kind of deterioration occurs is not solved to date. Hereinafter, we adopt one more criterion to eliminate the deteriorated data; i.e. $P_{NB_e} / \langle n_e \rangle < 5 \text{ MW} / 10^{19} \text{ m}^{-3}$.

Next, we compare the global energy confinement of the electrons in the hydrogen and

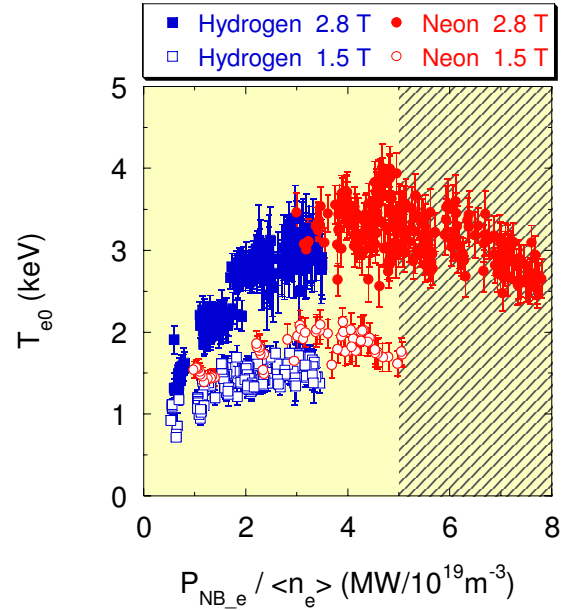


Fig. 2. Dependence of T_{e0} on $P_{NB_e} / \langle n_e \rangle$. Plotted are the data that satisfy the two criteria; $\langle n_e \rangle < 2 \times 10^{19} \text{ m}^{-3}$, and $P_{ei} / P_{NB} < 0.1$.

the heat transfer from the electrons to the ions, P_{ei} , should be considered carefully. The maximum P_{ei} reaches to 1 MW at $\langle n_e \rangle < 2 \times 10^{19} \text{ m}^{-3}$ and is not small enough to be neglected. Hereinafter, we eliminate the data that has $P_{ei} / P_{NB} > 0.1$, and neglect P_{ei} to reduce its influence.

The relation between T_{e0} and the electron heating power per an electron, $P_{NB_e} / \langle n_e \rangle$, is plotted in Fig. 2. In the range of $P_{NB_e} / \langle n_e \rangle < 5 \text{ MW} / 10^{19} \text{ m}^{-3}$, T_{e0} increases with $P_{NB_e} / \langle n_e \rangle$, and any particular

the neon plasmas. The non-dimensional regression analysis of the experimental electron energy confinement time, $\tau_{E_e}^{\text{exp}} (\equiv W_{e_kin} / P_{NB_e})$ is examined. In the non-dimensional form, $\tau_{E_e}^{\text{exp}}$ can be expressed as

$$\tau_{E_e}^{\text{exp}} \Omega_e \propto B_0 \tau_{E_e}^{\text{exp}} \propto (\rho_e^*)^\phi (\nu^*)^\gamma (\beta_e)^\eta, \quad (1)$$

where Ω_e is the electron gyro frequency, $\rho_e^* = \rho_e / a$ is the normalized electron gyro radius, ν^* is the collisionality, and β_e is the normalized electron pressure [2]. For the hydrogen data, however, the linear correlation coefficients of each components are 0.89, 0.35 and 0.54 for ρ_e^* , ν^* , and β_e , respectively. Here, we neglect the dependence on ν^* and β_e , since these are not strongly correlating with $\tau_{E_e}^{\text{exp}}$. Regression analysis with ρ_e^* alone gives;

$$B_0 \tau_{E_e}^{\text{exp}} (\text{H}) = 3.57 \times 10^{-13} (\rho_e^*)^{-2.74 \pm 0.07}. \quad (2)$$

As for the neon data, the linear correlation coefficients for each components are 0.91, 0.49 and 0.27 for ρ_e^* , ν^* , and β_e , respectively. Again, ν^* and β_e are not strongly correlating with $\tau_{E_e}^{\text{exp}}$. Regression analysis with ρ_e^* alone results in

$$B_0 \tau_{E_e}^{\text{exp}} (\text{Ne}) = 1.15 \times 10^{-12} (\rho_e^*)^{-2.61 \pm 0.09}. \quad (3)$$

In both of the hydrogen and the neon plasmas, $B_0 \tau_{E_e}^{\text{exp}}$ is strongly related to ρ_e^* and the exponents are identical within the standard deviations. These relations are plotted in Fig. 3 (a). This suggests that both plasmas have similar parameter dependence of the global electron energy confinement. The difference in the coefficients between Eqs. (2) and (3) is possibly due to the small ρ_e^* of $\sim 10^{-4}$ (note that even the small difference of 0.1 in the exponents causes an error of factor 2.5 in the coefficients). To compare the coefficients more accurately, we assume a model equation with the exponent of -2.7 ;

$$\tau_{E_e}^{\text{fit}} \Omega_e \propto B_0 \tau_{E_e}^{\text{fit}} \propto (\rho_e^*)^{-2.7}. \quad (4)$$

In the gyro-Bohm model, where micro-turbulences are considered as the cause of the anomalous energy transport [3, 4], the exponent of -3 is assumed, while it is -2 in the Bohm model, for example (note that ρ_i^* is used instead of ρ_e^* , in these models). Equation (4) can be rewritten using the conventional terms as below;

$$\tau_{E_e}^{\text{fit}} = C_0 a^{2.30} R^{0.574} B_0^{0.723} P_{NB_e}^{-0.574} \langle n_e \rangle^{0.574}, \quad (5)$$

where C_0 is the fitting parameter, and the units of each terms are; m, m, T, MW, and 10^{19} m^{-3} , for a , R , B_0 , P_{NB_e} , and $\langle n_e \rangle$, respectively. Fitting the data with Eq. (5), the distributions of

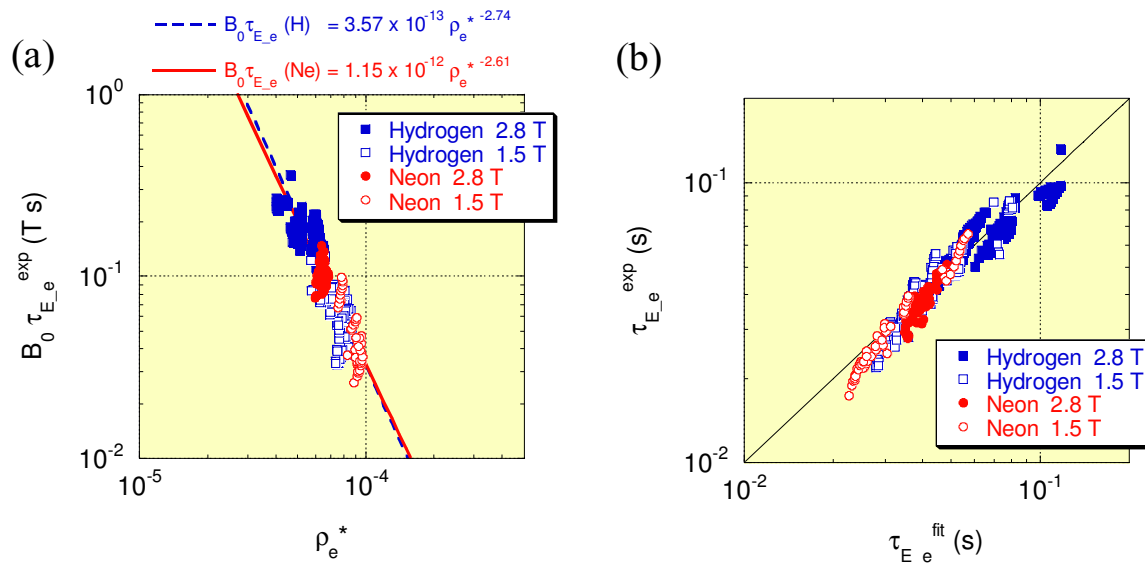


Fig. 3. (a) Dependence of $B_0 \tau_{E_e}^{\text{exp}}$ on ρ_e^* , and (b) the comparison of $\tau_{E_e}^{\text{exp}}$ and $\tau_{E_e}^{\text{fit}}$. Plotted are the data that satisfy the three criteria; $\langle n_e \rangle < 2 \times 10^{19} \text{ m}^{-3}$, $P_{\text{ci}} / P_{\text{NB}} < 0.1$, and $P_{\text{NB}_e} / \langle n_e \rangle < 5 \text{ MW} / 10^{19} \text{ m}^{-3}$.

$\tau_{E_e}^{\text{exp}}$ in the plasmas with different ion species can be compared. Using hydrogen dataset, $C_0 = 0.060 \pm 0.007$ is obtained, while $C_0 = 0.056 \pm 0.004$ is obtained with the neon dataset. In both cases, C_0 is identical within the standard deviations. Assuming $C_0 = 0.06$, $\tau_{E_e}^{\text{exp}}$ and $\tau_{E_e}^{\text{fit}}$ are compared in Fig. 3 (b). As is seen in the figure, $\tau_{E_e}^{\text{fit}}$ well reproduces $\tau_{E_e}^{\text{exp}}$, and its absolute value is similar in both of the hydrogen and the neon plasmas.

These results are contrastive to the Z-mode [5] and the RI-mode [6] in tokamaks, where a reduction of the electron thermal diffusivity induced by the impurity (including the neon) gas puff has been observed. In this study, however, parameter region is limited. Especially, the confinement deterioration at $P_{\text{NB}_e} / \langle n_e \rangle > 5 \text{ MW} / 10^{19} \text{ m}^{-3}$ is observed only in the neon plasmas. Whether this deterioration will also occur in the hydrogen plasmas, or not, should be examined in the future experiment. The energy confinement of the ions has not been treated in this study. To carry out the conclusive discussion on this, it is necessary to measure the ion temperature profile and the ion density profile.

References

- [1] U. Stroth et al., Nucl. Fusion **36**, 1063 (1996).
- [2] H. Yamada et al., Plasma Phys. Control. Fusion **43**, A55 (2001).
- [3] R. J. Goldston et al., Bull. Am. Phys. Soc. **34**, 1964 (1989).
- [4] M. Murakami et al., Phys. Fluids B **3**, 2261 (1991).
- [5] E. A. Lazarus et al., Nucl. Fusion **25**, 135 (1985).
- [6] G. R. McKee et al., Phys. Plasmas **7**, 1870 (2000).